

COMPUTATIONAL ANALYSIS OF MHD FLOW, HEAT AND MASS TRANSFER IN TRAPEZOIDAL POROUS CAVITY

by

Ramdane YOUNSI

Original scientific paper
UDC: 532.546:66.086.4:66.011
BIBLID: 0354-9836, 13 (2009), 1, 13-22
DOI:10.2298/TSCI0901013Y

Numerical simulations are conducted for two-dimensional steady-state double diffusive flow in a trapezoidal porous cavity, submitted to axial magnetic field. The Darcy equation, including Brinkmann and Forchheimer terms account for viscous and inertia effects, respectively is used for the momentum equation, and a SIMPLER algorithm, based on finite volume approach is used to solve the pressure-velocity coupling. An extensive series of numerical simulations is conducted in the range: $10^3 \leq Ra \leq 10^6$, $1 \leq Ha \leq 10^2$, $Da = 10^{-3}$, $N = 1$, and $Le = 10$. It is shown that the application of a transverse magnetic field normal to the flow direction decreases the Nusselt number and Sherwood number. Illustrative graphs are presented.

Key words: *double diffusion, porous media, heat and mass transfer, magneto-hydrodynamics, finite volume method*

Introduction

Double-diffusive natural convection in porous media has received considerable attention due to its numerous applications in geophysics and energy related engineering problems. Such types of applications include natural circulation in isothermal reservoirs, aquifers, porous insulation, heat storage beds, grain storage, extraction of geothermal energy, and thermal insulation design, *etc.* One important example of double-diffusive convection can be found in material solidify processes. Since solidification of alloys and crystals necessary involves the simultaneous flows of momentum, heat, and solute. The appearance of thermal and concentration gradients near the solid-liquid interface can causes a uniform density distribution and convection-diffusion motion there, which may have a profound effects on the solid structure as it is crystallized from the liquid state. Electromagnetic field has been used in the metal industry to control microstructures solidification and to reduce or eliminate natural convection in the melt. In crystal growth process, the objective is to adjust the process and characteristics of the magnetic filed in order to eliminate the deleterious unsteadiness in the melt motion and to achieve a steady melt motion which produces uniform and controllable dopant and contaminant concentrations in the crystal. A major advantage of a magnetic field is that it can be tailored to achieve different field strengths and orientations at different positions in the melt and at different stages during the growth of a crystal.

The combined heat and mass transfer in porous media is limited, because of complexities involved in double-diffusive natural convection. Most of previous studies in this topic use Darcy's law for solving flow within the porous medium. Natural convection of heat and mass

transfer in a square porous cavity subjected to constant temperature and concentration has been investigated by Trevisian *et al.* [1]. The authors use the Darcy's model for modeling the flow in porous medium. The numerical study has been carried out for a given range of Darcy-Rayleigh number, Lewis number, and buoyancy ratio. Lage [2] studied the effect of the convective inertia term on Benard convection in a porous medium. The author shows that inertia term included in the general momentum equation has no effect on the overall heat transfer. Agrawal *et al.* [3] discussed thermal and mass diffusion on hydromagnetic viscoelastic natural convection past an impulsively started infinite plate in the presence of a transverse magnetic field. Helmy [4] studied the unsteady laminar free convection flow of an electrically conducting fluid through a porous medium bounded by an infinite vertical plane surface of constant temperature. Shanker *et al.* [5] presented the effect of mass transfer on the MHD flow past an impulsively started infinite vertical plate. Ram *et al.* [6] studied the MHD free convection flow past an impulsive started vertical infinite plate when a strong magnetic field of uniform strength was applied transversely to the direction of flow. The first work in MHD using the state space approach was done by Ezzat [7-9], where the heated vertical plate problem was solved using a numerical inverse Laplace transform. Ezzat *et al.* [8] formulated the state space approach for the one-dimensional problem of viscoelastic magnetohydrodynamic unsteady free convection flow with the effects on a viscoelastic boundary layer flow with one relaxation time. Bian *et al.* [10] considered the interaction of an external magnetic field with convection currents in a porous medium. The porous medium was modeled according to Darcy's model. It is found that the application of a magnetic field, modifies the temperature and flow fields significantly. The purpose of the present paper is to study the double-diffusive natural convection flow behaviour and its effects on heat and mass transfer in a trapezoidal porous cavity submitted to transverse magnetic field. The flow is modeled using the generalized model of Darcy-Brinkman-Forchheimer. Thermosolutal heat transfer within trapezoidal cavity heated at the bottom and cooled at the inclined top part was investigated by Boussaid *et al.* [11]. The convective heat transport equation was solved by alternating direction implicit (ADI) method combined with a fourth-order compact Hermitian method. Natarajan *et al.* [12] analysed the natural convection flow within a trapezoidal enclosure where the bottom wall is heated (uniformly and non-uniformly) and vertical walls are cooled by means of a constant temperature bath whereas the top wall is well insulated. The consistent penalty finite element method has been used to solve the non-linear-coupled partial differential equations for flow and temperature fields with both uniform and non-uniform temperature distributions prescribed at the bottom wall. The effect of Prandtl number in the variation of local and average Nusselt numbers was found to be more significant for Prandtl numbers in the range 0.07-0.7 than 10-100. Baytas *et al.* [13] studied the natural convection flow behaviour and its effects on the heat transfer and temperature distribution within a non-rectangular enclosure filled with a porous medium and which is inclined with an arbitrary angle from the vertical. The enclosure chosen is of trapezoidal cross-section with paralleled cylindrical top and bottom walls at different temperatures and plane adiabatic sidewalls. Flow and heat transfer characteristics (stream lines, isotherms, and average Nusselt numbers) are investigated for a wide range values of the Rayleigh number, inclined angle and cavity aspect ratio.

Problem definition and governing equations

The problem considered is a two-dimensional natural convection flow in a trapezoidal porous cavity filled with a binary fluid, see fig. 1. Different types of boundary conditions have been employed. Dirichlet conditions are prescribed along the top and the bottom surfaces for temperature and concentration. On both left and right surfaces, Neuman, *i. e.*, zero gradient con-

ditions are assigned to temperature and concentration. A uniform magnetic field is applied transversally. Both velocity components are equal to zero on boundaries.

For simpler analysis, some assumptions are made:

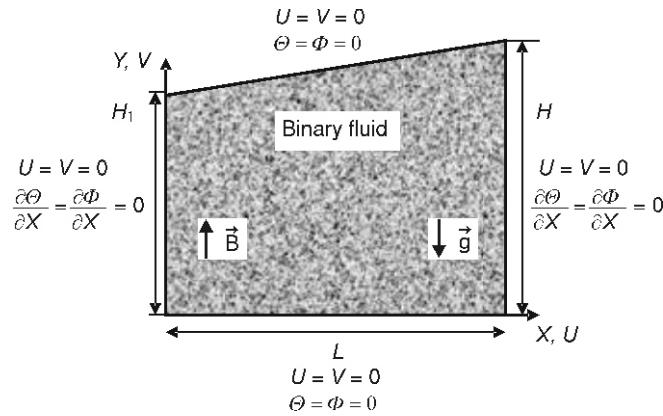


Figure 1. The physical model and coordinate system

- the binary fluid is assumed to be Newtonian incompressible and to satisfy the Boussinesq approximation,
- the flow in the cavity is laminar and two-dimensional,
- the porous medium is supposed to be isotropic homogeneous and in thermodynamic equilibrium with the binary fluid,
- the Soret and Dufour effects are neglected, and
- the magnetic Reynolds number of the fluid is neglected.

Then applying the theorem of conservation and introducing the dimensionless parameters as given below:

$$(X, Y) = \frac{(x, y)}{H}, (U, V) = \frac{(u, v)}{\frac{\alpha_p}{H} \sqrt{\text{Ra Pr}}}, \tau = \frac{t}{\frac{H^2}{\alpha_p}} \sqrt{\text{Ra Pr}}, \lambda = \frac{(\rho C_p)_p}{(\rho C_p)_f}$$

$$\Theta = \frac{T - \frac{T_1 + T_2}{2}}{T_1 - T_2}, \Phi = \frac{C - \frac{C_1 + C_2}{2}}{C_1 - C_2}, P = \frac{\varepsilon^2 H^2 p}{\rho_f \alpha_p^2 (\text{Ra Pr})}$$

We obtain the following dimensionless governing equations as given also by Lage [2]:

- continuity equation

$$\frac{\partial U}{\partial X} + \frac{\partial V}{\partial Y} = 0 \tag{1}$$

- X-momentum equation

$$\frac{1}{\varepsilon} \frac{\partial U}{\partial \tau} + (\vec{V} \cdot \nabla) U = -\frac{\partial P}{\partial X} + \varepsilon \sqrt{\frac{\text{Pr}}{\text{Ra}}} \nabla^2 U + \frac{C_f \varepsilon^2}{\sqrt{\text{Da}}} |\vec{V}| U - \frac{\varepsilon^2}{\text{Da}} \sqrt{\frac{\text{Pr}}{\text{Ra}}} U - \text{Ha}^2 \sqrt{\frac{\text{Pr}}{\text{Ra}}} U \tag{2}$$

- Y-momentum equation

$$\frac{1}{\varepsilon} \frac{\partial V}{\partial \tau} + (\vec{V} \cdot \nabla) V = -\frac{\partial P}{\partial Y} + \varepsilon \sqrt{\frac{\text{Pr}}{\text{Ra}}} \nabla^2 V + \frac{C_f \varepsilon^2}{\sqrt{\text{Da}}} |\vec{V}| V - \frac{\varepsilon^2}{\text{Da}} \sqrt{\frac{\text{Pr}}{\text{Ra}}} V - \varepsilon^2 (\Theta - N\Phi) \tag{3}$$

– energy equation

$$\frac{1}{\lambda} \frac{\partial \Theta}{\partial \tau} + (\vec{V} \cdot \nabla) \Theta = \frac{1}{\sqrt{\text{Ra Pr}}} \nabla^2 \Theta \quad (4)$$

– species equation

$$\varepsilon \frac{\partial \Phi}{\partial \tau} + (\vec{V} \cdot \nabla) \Phi = \frac{1}{\text{Le} \sqrt{\text{Re Pr}}} \nabla^2 \Phi \quad (5)$$

The initial and boundary conditions for the dimensionless equations are:

– initial condition (at $\tau = 0$)

$$\begin{aligned} \Theta &= \Theta_0 = 0 \\ \Phi &= \Phi_0 = 0 \quad \text{for } 0 \leq Y \leq 1 \quad \text{and } 0 \leq X \leq \frac{1}{A} \\ U &= V = 0 \end{aligned} \quad (6)$$

– boundary conditions

$$\begin{aligned} \Theta &= \Phi = 1, \quad U = V = 0 \quad \text{for } Y = 0 \quad \text{and } 0 \leq X \leq \frac{1}{A} \\ \Theta &= \Phi = 0, \quad U = V = 0 \quad \text{for } Y = aX + b \quad \text{and } 0 \leq X \leq \frac{1}{A} \\ \frac{\partial \Theta}{\partial X} = \frac{\partial \Phi}{\partial X} &= 0, \quad U = V = 0 \quad \text{for } X = 0 \quad \text{and } 0 \leq Y \leq b \\ \frac{\partial \Theta}{\partial X} = \frac{\partial \Phi}{\partial X} &= 0, \quad U = V = 0 \quad \text{for } X = \frac{1}{A} \quad \text{and } 0 \leq Y \leq 1 \end{aligned} \quad (7)$$

Numerical procedure

The coupled transient equations are solved to obtain a steady-state solution. When a convergent result is approached, the transient terms vanish and the steady-state equations are solved. The differential equations are discretised in space with the control-volume finite difference method described by Patankar [14]. The resulting finite difference scheme has the form:

$$A_p \phi_p = A_E \phi_W + A_W \phi_N + A_N \phi_S + A_S \phi_S + S \quad (8)$$

Expressions for the coefficients in eq. (8) may be found in reference [14]. The advection-diffusion part of the coefficients A_E , A_W , A_N , and A_S is modified for stability according to the power law scheme. The source term S includes the values of at previous time step. The discretisation technique is well known and S detailed description is not needed. The linear system derived from the conservation equations are solved using line-by-line method. As the momentum equation is formulated in terms of the primitive variables (U , V , P) the iterative procedure includes a pressure correction calculation method to solve the pressure-velocity coupling (the SIMPLER technique [14]). The simulations are generally performed using 101×101 sinusoidal grid. It is realized that this relatively coarse grid is adequate to resolve all details of the flow structures in the cavity. The selected mesh size should only be viewed as a compromise between accuracy and computational time. The convergence of the numerical solution was monitored locally. The max-norm was used for the velocity components U , V , temperature Θ , and concentration Φ the convergence criterion at each time step is:

$$\max \left| \frac{(U, V, \Theta, \Phi)^{i+1} - (U, V, \Theta, \Phi)^i}{(U, V, \Theta, \Phi)^i} \right| \leq 10^{-5} \quad (9)$$

in which i and $i + 1$ denote two consecutive iterations at the same time step.

The average heat and mass transfer at the walls are given in dimensionless terms by the Nusselt and Sherwood numbers defined as:

$$Nu_0 = \int_0^1 \frac{\partial \Theta}{\partial Y} dX, \quad Sh_0 = \int_0^1 \frac{\partial \Phi}{\partial Y} dX \quad (10)$$

Test validation

The numerical accuracy of the present study has been checked over a large number of purely thermal convection in a square fully porous cavity, the results has been compared with the results of earlier studies in tabs. 1 and 2, for the Darcy and combined Darcy-Brinkman representation of the porous medium flow. The validation is performed using 81 × 81 sinusoidal grid. It may be seen from the results, that the agreement with references (Lauriat *et al.* [15]; Nithiarasu *et al.* [16]) is excellent in most cases. Indeed, our results present a difference less than 2% in comparison with Nithiarasu *et al.* [16] results.

Table 1. Darcy model (pure heat transfer, N = 0)

Nu ₀			
Ra* = Ra _t Da	Lauriat <i>et al.</i> [15]	Nithiarasu <i>et al.</i> [16]	Present work
10	1.07	1.08	1.06
50	–	1.958	1.936
100	3.09	3.2	2.98
500	–	8.38	8.32
1000	13.41	12.514	12.49

Table 2. Darcy-Brinkman model (pure heat transfer, N = 0, Pr = 1)

Nu ₀				
Ra* = Ra _t Da	Da	Lauriat <i>et al.</i> [15]	Nithiarasu <i>et al.</i> [16]	Present work
10	10 ⁻⁶	1.07	1.08	1.06
100	10 ⁻⁶	3.06	3.00	2.98
1000	10 ⁻⁶	13.2	12.25	12.11
10	10 ⁻²	1.02	1.02	0.99
100	10 ⁻²	1.7	1.71	1.68
1000	10 ⁻²	4.26	4.26	4.24

Results and discussion

The objective in this section is to present a sample of results in order to illustrate the effect of Rayleigh number (Ra) and Hartman number (Ha) on the cell formation processes and heat and mass transfer characteristics. This study is limited to fluid with Prandtl number Pr = 0.149 that correspond to a titanium based alloy and Lewis number Le = 10. The conductivity ratio is λ = 1

and the representative porosity is fixed to $\varepsilon = 0.4$ for porous medium. The inertia parameter C_f is calculated using the Ergun model [17] $C_f = 1.75/(150\varepsilon^3)^{1/2}$ which means that in the present case $C_f = 0.56$.

Influence of Rayleigh number

In fig. 2, the effect of Rayleigh number is illustrated for $A = 1$, $Da = 10^{-5}$, $N = 1$, and $Le = 10$. The results are presented in terms of velocity vectors, isotherms and iso-concentration contours for different values of Rayleigh number. The flow directions in the graphs can be easily identified. Due to the thermal and solutal boundary conditions considered here, the bottom wall has a higher temperature and concentration as the top inclined wall. As a result, the direction of the flow is counterclockwise. As the Rayleigh number is increased, both temperature and solutal buoyancy are augmenting each other and thus they accelerate the flow counterclockwise.

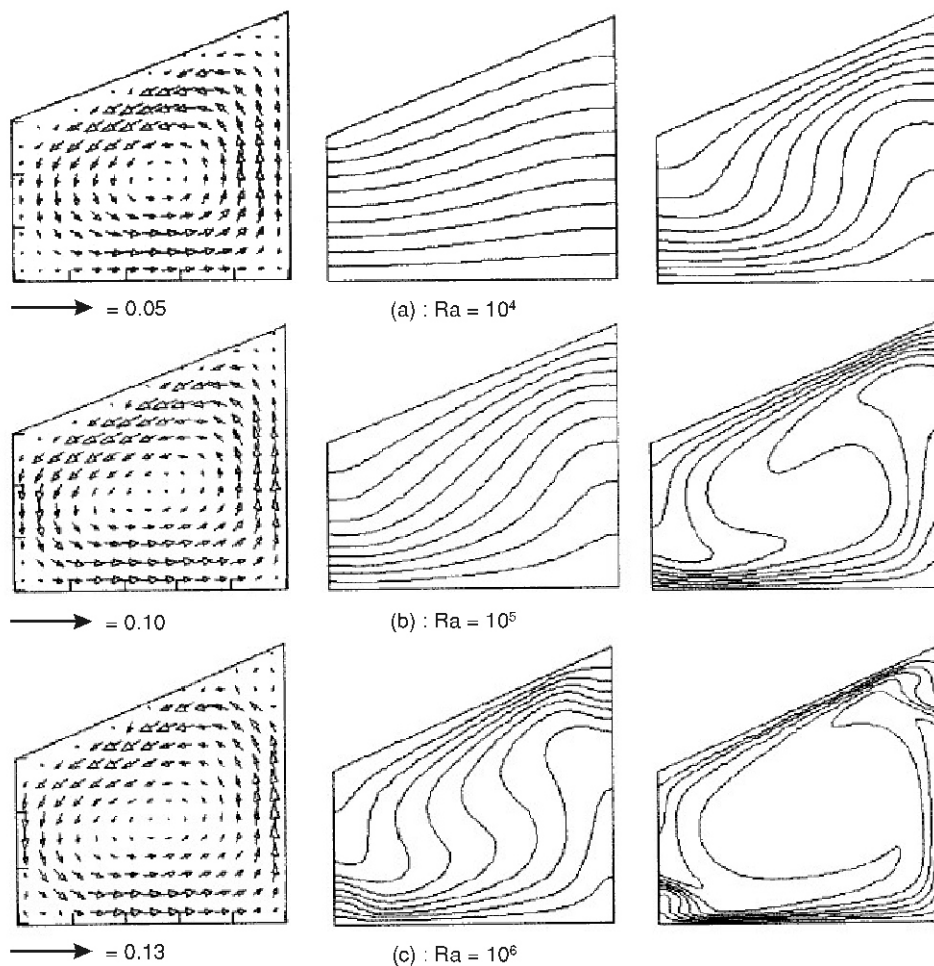


Figure 2. Velocity-vectors, isotherms, and isoconcentrations vs. Rayleigh number; $Pr = 0.149$
 $Ha = 0$, $Da = 10^{-5}$, $N = 1$, $Le = 10$

Influence of Hartman number

Figure 3 illustrates typical streamlines, velocity vectors, isotherms, and concentration lines for $Ra = 10^5$, $Da = 10^{-5}$, $Pr = 0.149$, $Le = 10$, $N = 1$, and $Ha = 0, 40$, and 80 , respectively. The influence of a magnetic field is apparent from this figure. Figure 3a shows the results obtained for $Ha = 0$ "absence of magnetic field". The flow, isotherms and isoconcentrations are similar to those obtained by other investigators [18]. The resulting flow regime is characterized by a boundary layer of constant thickness. Also, the parallelism of the flow and the existence of linear thermal and solutal stratification are clearly illustrated. Due to the thermal and solutal boundary conditions considered here, the bottom wall has a higher temperature and concentration as the top inclined wall. As a result, the direction of the flow is counter clockwise. When the magnetic field is applied, the flow recalculation is progressively inhibited by the retarding effect of the electromagnetic body force (figs. 3b and 3c). More quantitative comparison are presented

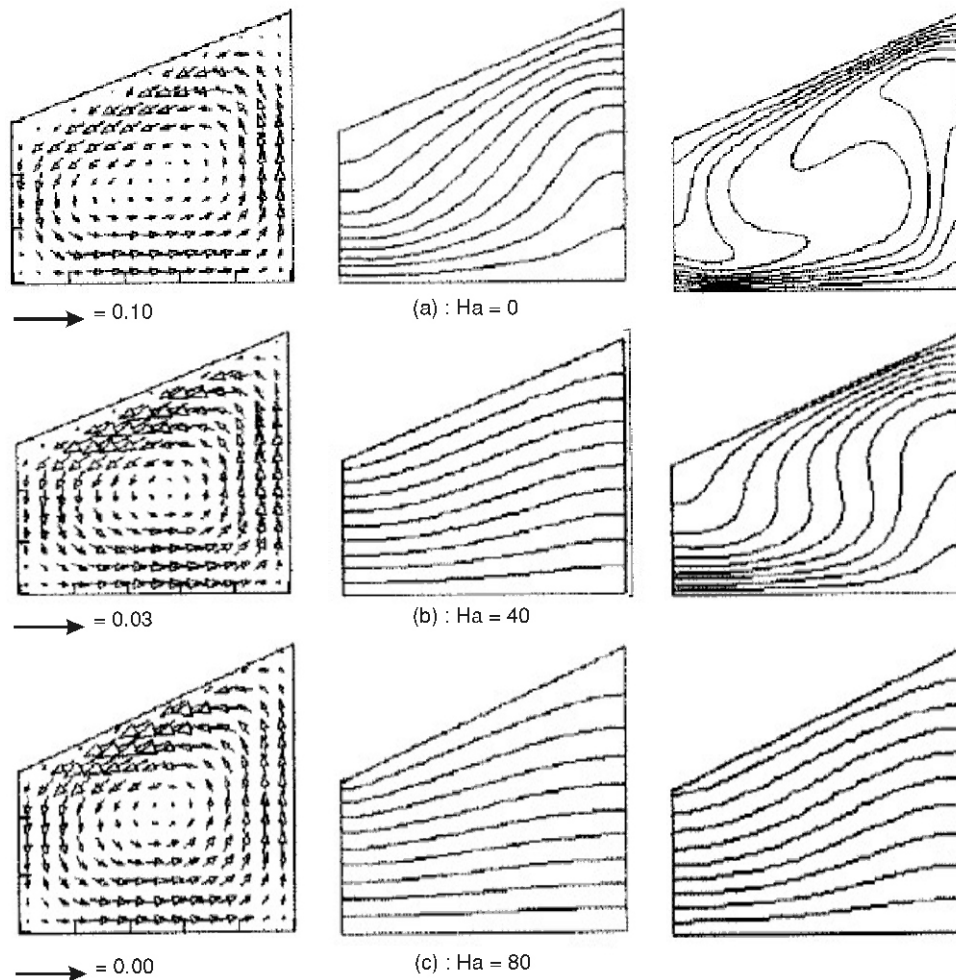


Figure 3. Velocity-vectors, isotherms, and isoconcentrations vs. Hartman number; $Pr = 0.149$, $Ra = 10^5$, $Da = 10^{-5}$, $N = 1$, $Le = 10$

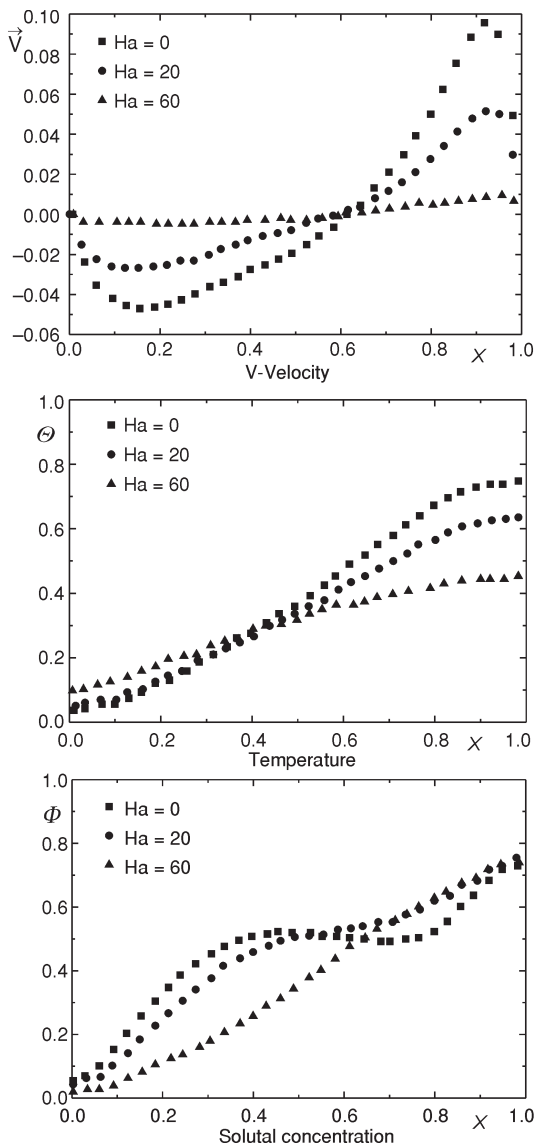


Figure 4. Effect of Hartman number on solution profiles along midplane; $Y = 0.5$, $Pr = 0.149$, $Ra = 10^5$, $Da = 10^{-5}$, $N = 1$, $Le = 10$

here in terms of \vec{V} -velocity, temperature, and solute profiles. All the profiles are plotted along the middle horizontal line of the enclosure, *i. e.*, along the line of $Y = 0.5$.

Figure 4 compare profiles obtained for $Da = 10^{-5}$ at different Hartman numbers $Ha = 0, 20$, and 60 . The effect of Hartman number on the convection field is well reflected by the progressive reduction of the velocity, temperature and solute concentration gradients as the Hartman number is increased.

Another view of the effect of Hartman on heat and mass transfer is found in fig. 5, where Nusselt and Sherwood numbers are plotted as a function of Ha . The analysis of this figure indicates that for small values of Ha , the boundary layer regime prevails. As the Hartman number increases, the electromagnetic body force increases which suppresses progressively the strength of the convective motion, and thus boundary layer regime is followed by the double diffusive regime for which Nusselt and Sherwood numbers tend to one.

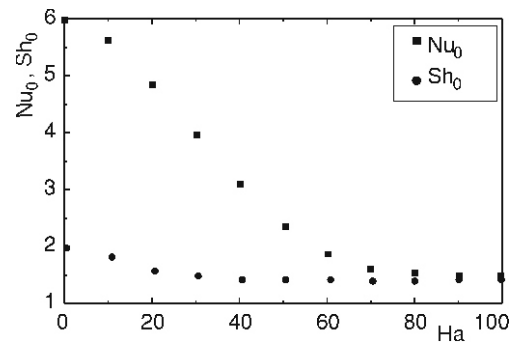


Figure 5. Effect of Hartman number on the Nusselt and Sherwood numbers; $Pr = 0.149$, $Ra = 10^5$, $Da = 10^{-5}$, $N = 1$, $Le = 10$

Conclusions

Double-diffusive natural convection in trapezoidal porous cavity, with transverse magnetic field has been studied numerically. The present model has been successfully validated with results of references. The convective of heat and mass transfer is strongly inhibited with increasing magnetic field. The overall heat and mass transfers decrease for increasing magnetic field.

The present analysis is focused on the influence of a limited number of dimensionless parameters. As an extension of this work, it is particularly relevant to take into account the buoyancy ratio (N), the Prandtl number (Pr), the Lewis number (Le), and correlate heat and mass transfer.

Nomenclature

A	– aspect ratio ($= H/L$), [–]	X, Y	– dimensionless Cartesian coordinate, [–]
\vec{B}	– magnetic field, [T]	x, y	– Cartesian coordinate, [m]
C	– concentration, [kgm^{-3}]	<i>Greek letters</i>	
ΔC	– concentration difference between plates ($= C_1 - C_2$), [kgm^{-3}]	α	– thermal diffusivity, [m^2s^{-1}]
C_f	– inertial coefficient, [–]	β_S	– isobaric coefficient of solutal expansion fluid, [–]
C_p	– specific heat at constant pressure, [$\text{Jkg}^{-1}\text{K}^{-1}$]	β_T	– isobaric coefficient of thermal expansion fluid, [–]
D	– mass diffusivity, [m^2s^{-1}]	ε	– porous media porosity, [–]
Da	– Darcy number ($= KH^2$), [–]	Θ	– dimensionless temperature, [–]
Gr_S	– solutal Grashof number ($= g\beta_S\Delta TH^3/\nu^2$), [–]	λ	– conductivity ratio
Gr_T	– thermal Grashof number ($= g\beta_T\Delta TH^3/\nu^2$), [–]	ν	– kinematic viscosity, [m^2s^{-1}]
\vec{g}	– acceleration due to gravity, [ms^{-2}]	ρ	– density, [kgm^{-3}]
H	– cavity high, [m]	σ	– electrical conductivity of the liquid, [sm^{-1}]
Ha	– Hartman number [$= \vec{B}\varepsilon(\sigma H/\nu)^{1/2}$], [–]	τ	– dimensionless time, [–]
K	– permeability, [m^2]	Φ	– dimensionless concentration { $= [C - (C_1 + C_2)/2]/\Delta C$ }, [–]
L	– cavity width, [m]	<i>Subscripts</i>	
Le	– Lewis number ($= Pr Sc$), [–]	f	– fluid
N	– buoyancy ratio ($= Gr_S/Gr_T$), [–]	p	– porous media
Nu_0	– overall Nusselt number, [–]	1	– heated surface
Pr	– Prandtl number ($= \nu/\alpha$)	2	– cooled surface
Ra	– Rayleigh number ($= Gr_T Pr$), [–]	0	– average value
Sc	– Schmidt number ($= \nu/D$), [–]	<i>Superscripts</i>	
Sh_0	– overall Sherwood number, [–]	i	– time iteration
T	– temperature, [K]		
ΔT	– temperature difference between plates ($= T_1 - T_2$), [K]		
t	– time, [s]		
U, V	– dimensionless velocity in (X, Y) direction, [–]		
u, v	– velocities in x, y direction, [ms^{-1}]		
\vec{V}	– velocity vector, [ms^{-1}]		

References

- [1] Trevisan, O., Bejan, A., Natural Convection with Combined Heat and Mass Transfer Effects in a Porous Medium, *Int. J. Heat and Mass Transfer*, 28 (1985), 8, pp. 1597-1611
- [2] Lage, J. L., Effect of the Convective Inertia Term on Bénard Convection in a Porous Medium, *Numerical Heat Transfer*, 22 (1992), 4, pp. 469-485
- [3] Agrawal, A. K., Samria, N. K., Gupta, S. N., Combined Buoyancy Effects of Thermal and Mass Diffusion on Hydromagnetic Viscoelastic Natural Convection Flow Past an Accelerated Infinite Plate, *J. En. Heat Mass Tran.*, 20 (1998), 2, pp. 35-42
- [4] Helmy, K. A., MHD Unsteady Free Convection Flow Past a Vertical Porous Plate, *ZAMM*, 78 (1998), 4, pp. 255-270
- [5] Shanker, B., Kishan, N., The Effects of Mass Transfer on the MHD Flow Past an Impulsively Started Infinite Vertical Plate with Variable Temperature or Constant Heat Flux, *J. En. Heat Mass Tran.*, 19 (1987), 1, pp. 273-278
- [6] Ram, P. C., Takhar, H. S., MHD Free Convection from an Infinite Vertical Plate in a Rotating Fluid with Hall and Ion Slip Currents, *Fluid Dyn Res*, 11 (1993), 3, pp. 99-105

- [7] Ezzat, M. A., State Space Approach to Unsteady Two-Dimensional Free Convection Flow Through a Porous Medium, *Can. J. Phys.*, 1 (1994), 5-6, pp. 311-317
- [8] Ezzat, M. A., *et al.*, State Space Formulation to Viscoelastic Magnetohydrodynamic Unsteady Free Convection through a Porous Medium, *Acta Mech.*, 119 (1996), 5-6, pp. 147-164
- [9] Ezzat, M. A., Abd-Elaal, M., Free Convection Effects on a Viscoelastic Boundary Layer Flow with One Relaxation Time through a Porous Medium. *J. Franklin Inst.*, 334 (1997), 4, pp. 685-709
- [10] Bian, W., Vasseur, P., Bilgen, E., Meng, F., Effect of Electromagnetic Field on Natural Convection in Inclined Porous Layer, *J. Heat Transfer and Fluid Flow*, 17 (1996), 1, pp.36-44
- [11] Boussaid, M., Djerrada, A., Bouhadeh, M., Thermosolutal Transfer within Trapezoidal Cavity, *Numerical Heat Transfer, A* 43 (2003), 4, pp. 431-448
- [12] Natarajan, E., Basak, T., Roy, S., Natural Convection Flows in a Trapezoidal Enclosure with Uniform and Non-Uniform Heating of Bottom Wall, *International Journal of Heat and Mass Transfer*, 51 (2008), 3-4, pp. 747-756
- [13] Baytas, A. C., Pop, I., Natural Convection in a Trapezoidal Enclosure Filled with a Porous Medium, *International Journal of Engineering Science*, 39 (2001), 2, pp. 125-134
- [14] Patankar, S. V., Numerical Heat Transfer and Fluid Flow, Hemisphere Publ. Comp., McGrawHill, New York, USA, 1980
- [15] Lauriat, G., Prasad, V., Non-Darcian Effects on Natural Convection in a Vertical Porous Enclosure, *Int. J. Heat and Mass Transfer*, 32 (1989), 11, pp. 2135-2148
- [16] Nithiarasu, P., Seetharamu, K. N., Sundararajan, T., Double-Diffusive Natural Convection in an Enclosure Filled with Fluid-Saturated Porous Medium: a Generalized Non-Darcy Approach, *Numerical Heat Transfer, Part A*, 30 (1996), 4, pp. 413-426
- [17] Ergun, S., Fluid Flow through Packed Columns, *Chem. Eng. Progr.*, 48 (1952), 2, pp. 89-94
- [18] Kimura, S., Bejan, A., The Boundary Layer Natural Convection Regime in a Rectangular Cavity with Uniform Heat Flux From the Side, *J. of Heat Transfer*, 106 (1984), 1, pp. 98-103

Author's affiliation:

R. Younsi
Applied Sciences Department,
University of Quebec at Chicoutimi
555, Boul. de l'Université
G7H 2B1 Chicoutimi, Qc, Canada

E-mail: ryounsi@uqac.ca